Published in final edited form as:
Neuroscience. 2007 May 25; 146(3): 1053–1061.

Comparison of in vivo and in vitro gene expression profiles in subventricular zone neural progenitor cells from the adult mouse after middle cerebral artery occlusion

Xian Shuang Liu[1], **Zheng Gang Zhang**[1], **Rui Lan Zhang**[1], **Sara R. Gregg**[1], **He Meng**[1], and **Michael Chopp**[1,2]

1*Department of Neurology, Henry Ford Health Sciences Center, Detroit, MI 48202*

2*Department of Physics, Oakland University, Rochester, MI 48309*

Abstract

Stroke stimulates neurogenesis in the adult rodent brain. The molecules that mediate stroke-induced neurogenesis are not definitely known. Using microarrays containing approximately 400 known genes associated with stem cell and angiogenesis, we compared transcriptional profiles of subventricular zone (SVZ) tissue with cultured neural progenitor cells isolated from the SVZ 7 days after ischemic stroke in the adult mouse. In SVZ tissue, we found that stroke upregulated 58 genes which are involved in multiple signaling pathways during embryonic development, suggesting that stroke recaptures embryonic molecular signals. In neural progenitor cells cultured in growth medium, 23 gene expressions were increased after stroke and 8 out of 23 genes overlapped with upregulated genes in stroke SVZ tissue. Expression alterations of selected genes were confirmed by real-time RT-PCR and immunohistochemistry. These in vivo and in vitro data provide new insight into the genetic program of adult SVZ neural progenitor cells after stroke and demonstrate gene expression differences between SVZ tissue and cultured SVZ cells.

Keywords

Neurogenesis; subventricular zone (SVZ); microarray; progenitor cell; stroke

Introduction

Cerebral impairment caused by ischemic stroke prompts the proliferation, migration and differentiation of SVZ progenitor cells in the adult brain (Arvidsson et al., 2002;Parent et al., 2002;Jin et al., 2003;Zhang et al., 2004a;Zhang et al., 2004b). However the molecular basis underlying these neurogenic events remains unknown. The identification of molecular pathways and potential modulators of SVZ progenitor cells after stroke is not only critical for the development of stem cell based medical therapies, but also vital for the pharmacological promotion of neurogenesis.

Applying microarrays, several groups have shown complex gene profiles in cultured SVZ neurospheres and SVZ tissue under different conditions (Gurok et al., 2004;Pennartz et al.,

Please send all correspondence to: Zheng Gang Zhang, MD, Ph.D Department of Neurology Henry Ford Hospital 2799 West Grand Boulevard Detroit, MI 48202 Tel: 313-916-5456 Fax 313-916-1318 Email: zhazh@neuro.hfh.edu

2004;Lim et al., 2006). In cultured SVZ neurospheres, Gurok et al. measured gene expression changes during the course of neural progenitor cell differentiation (Gurok et al., 2004). Lim et al. measured in vivo gene expression profiles of adult SVZ tissue and demonstrated RNA splicing and chromatin remodeling as prominent processes for adult neurogenesis (Lim et al., 2006). These in vivo and in vitro studies provide valuable information on gene profiling of SVZ cells from the adult animal.

In the present study, we analyzed the transcriptional patterns of SVZ neural progenitor cells in vivo and in vitro after middle cerebral artery occlusion (MCAo) by means of microarrays. Our data demonstrate that stroke significantly alters gene profile expression and there are distinct differences in gene expression between SVZ tissue and cultured SVZ cells.

Materials and Methods

Animal model of MCAo

Male C57BL/6J mice (3 to 4 months) were employed in this study. The right middle cerebral artery (MCA) was occluded by placement of an embolus at the origin of the MCA, as previously described (Zhang et al., 1997). MCAo evokes a peak increase of neurogenesis 7 days after stroke (Zhang et al., 2004b;Zhang et al., 2001). Therefore, all mice were sacrificed 7 days after MCAo.

Neurosphere culture and tissue samples

SVZ neural progenitor cells were dissociated from normal (n=3) and MCAo mice (n=3), as previously reported (Zhang et al., 2004a;Reynolds et al., 1992;Chiasson et al., 1999;Morshead et al., 2002). Briefly, brain localized to bregma 2.2 to −0.3 mm was cut into a coronal section and the SVZ (2 mm width) from the lateral wall of the lateral ventricle was aseptically removed (Fig. 1A). The ependymal cells were not included. The cells were plated at a density of 2×10^4 cells per milliliter in growth medium which includes DMEM/F-12 medium (Invitrogen Corporation, Carlsbad, CA, USA), epidermal growth factor (EGF, 20 ng/ml, R&D System, Minneapolis, MN, USA), and basic fibroblast growth factor (bFGF, 20 ng/ml, R&D System, Minneapolis, MN, USA). SVZ cells were retained in a CO_2 incubator for 7 days and processed for microarray and RT-PCR analysis. SVZ tissue isolated from the ipsilateral hemispheres of rats subjected to MCAo (n=3) and hemispheres of normal rats (n=3), were pooled and stored at −80°C freezer until used in the microarray assay.

RNA isolation and gene expression microarray

Total RNAs from SVZ tissue and neurospheres were extracted using an RNeasy spin column purification kit (Qiagen, Valencia, CA, USA) in accordance with the manufacturer's procedure. To remove possible genomic DNA contamination, RNase-free DNase was used during the RNA purification steps.

The non-radioactive GEArray Q series cDNA expression array filters (MM-601.2N; SuperArray Incorporation, Frederick, MD, USA) were used and hybridization procedures were performed according to manufacturer's instructions. The biotin dUTP-labeled cDNA probes (biotin UTP-labeled oligo probes were applied in Oligo GEArray) were specifically generated in the presence of a designed set of gene-specific primers using total RNA (4 g) and 1l reverse transcriptase. The array filters were hybridized with biotin-labeled probes at 60°C for 17 hr. The filters were then washed twice with 2× saline sodium citrate buffer (SSC)/1% sodium dodecyl sulfate (SDS) and then twice with 0.1 x SSC/1% SDS at 60°C for 15 min each. Chemiluminescent detection steps were performed by subsequent incubation of the filters with alkaline phosphatase-conjugated streptavidin and CDP-Star substrate.

Data processing

For quantification, intensity of spots was measured using GEArray Expression Analysis Suite software (http://GEAsuite.superarray.com, SuperArray Incorporation, USA). Briefly, the lowest density spot on the array was found, and the average density across that spot was used as the background correction setting. Array spots were considered "present" only if genes were between the 25% and 75% quartile for normalization. To reduce the contamination by adjacent spots, "clover on" mode was used, which considers the four individual spots as a form of border for the capture of expression data. Total density was divided by the number of pixels to obtain average intensities that were used to compare gene expression levels between control and MCAo groups.

Reverse transcription and Quantitative real-time RT-PCR

Total RNAs isolated from SVZ tissue (n=6 rats) and cultured SVZ cells (n=4 rats) were processed by reverse-transcription. Real-time PCR was performed in ABI Prism 7700 Sequence Detection System (Applied Biosystems, Foster City, CA, USA) by using SYBR Green PCR Master Mix (Applied Biosystems) with 3-stage program parameters provided by the manufacturer, as follows: 2 min at 50°C to require optimal AmpErase uracil-N-glycosylase activity, 10 min at 95°C to activate AmpliTaq Gold DNA polymerase, and then each cycle 15 s at 95°C, 1 min at 60°C for 50 cycles. 2 min at 50°C, 10 min at 95°C, and then 40 cycles of 15 s at 95°C and 1 min at 60°C. Table 1 lists primers (Invitrogen Incorporation, Carlsbad, CA, USA) specific for the genes examined in the present study. Each sample was tested in triplicate and data obtained from three independent experiments were expressed as a subtraction of the quantity of specific transcripts to the quantity of the control gene (β-actin) in mean arbitrary units. CT values were quantified by the $2^{-\Delta\Delta Ct}$ method (Livak and Schmittgen, 2001).

Immunohistochemistry and immunocytochemistry

For immunohistochemistry, frozen sections were air-dried for 30 seconds, washed with PBS three times (5 min each), followed by fixation with 4% paraformaldehyde or acetone for 20 min at room temperature, and then blocked with 1% bovine serum aluminum (BSA) in PBS for 30 min. The following primary antibodies were applied for 1 hr at room temperature: goat polyclonal antibody against, mouse monoclonal antibody against Tenascin C (1:500, Abcam, Cambridge, MA, USA). After three washes in PBS (5 min each), biotinylated secondary antibodies (1:200, Vector, Burlingame, CA, USA) were applied for 30 min at room temperature. The reaction product was detected using 3'-3'-diaminobenzidine-tetrahydrochloride (DAB, Sigma, St. Louis, MO, USA). Omitting primary antibodies was used as a negative control.

For double immunofluorescence, brain sections were incubated overnight in a mixture of two primary antibodies raised in different species (ie, rabbit anti-GFAP, mouse anti-nestin and mouse anti-Tuj1). Species-specific CY3-and FITC-conjugated secondary antibodies (Jackson ImmunoResearch, West Grove, PA, USA) were used to visualize double-fluorescent immunostaining with Axioplan 2 fluorescent microscope (Carl Zeiss, Thornwood, NY, USA). Confocal microscopy was performed with a LSM 510 Meta (Carl Zeiss, Thornwood, NY, USA) and images were obtained at 2.2-m optical sections. Specificity of immunostaining was confirmed by omitting the primary antibodies.

Quantification

Semi-quantitative measurements of immunoreactive cells were performed according to our previously published methods (Zhang et al., 1999;Zhang et al., 2005). Briefly, immunoreactive cells in the non-stroke and stroke SVZ were digitized under a 40x objective (BX40; Olympus Optical) using a 3-CCD color video camera (DXC-970MD; Sony, Tokyo, Japan) interfaced

with an MCID image analysis system. The data are presented as a percentage of positive immunoreactivity area within the total SVZ area (pixel).

Statistical analysis

Student's t test was performed to compare immunoreactive cells in the SVZ between the non-stroke and stroke groups. The data are presented as mean ± SD; $P < 0.05$ was taken as a significant difference.

Results

General transcription profiles in SVZ neurospheres and SVZ tissue

To analyze genes involved in neurogenesis and angiogenesis after stroke, we employed the GEArray S Series Mouse Stem Cell Gene Array containing 258 known genes and the Oligo GEArray Mouse Angiogenesis Microarray containing 113 known genes (www.superarray.com). Figures 1 demonstrated gene profiles in MCAo and normal SVZ tissue from representative mouse stem cell gene arrays. To quantify the gene expression, all clones with more than 1.5 fold estimated differences were subjected to further evaluation. This threshold is based on a statistical analysis using online software provided by Superarray Inc, which has been widely employed (Campos et al, 2003).

In SVZ tissue and cultured SVZ neural progenitor cells obtained from mice subjected to MCAo, 58 and 23, respectively, of 371 genes were upregulated compared with SVZ tissue and SVZ neural progenitor cells obtained from normal mice (Fig. 1, 2 and Table 2, 3). Many genes are associated with the development of neural progenitor cells. Eight additional novel genes upregulated by MCAo overlapped between SVZ tissue and cultured SVZ cells (Table 2, 3), which included Hif 1α, a transcription factor that is essential for adaptive responses of the cell to hypoxia (Ran et al., 2005;Sharp et al., 2004).

Comparison of expression profiles between SVZ tissue and cultured SVZ neurospheres induced by MCAo

To identify the difference in gene expression profiles after MCAo, specific gene subfamilies were compared. Fibroblast growth factors (FGFs) are multifunctional signaling proteins that regulate developmental processes and adult physiology. Compared with normal SVZ, we found that multiple FGF subtypes and FGF receptor were upregulated in MCAo SVZ tissue (Table 2). However, FGF subtype genes were not upregulated in cultured SVZ neural progenitor cells (Table 3).

Integrins are cell surface receptors involved in cell-cell and cell-extra cellular matrix interactions (Campos LS, 2005). Several integrins were upregulated in MCAo SVZ tissue (Table 2), whereas MCAo did not strikingly increase integrin expression in cultured neural progenitor cells (Table 3). In addition, several other matrix molecules, for example intercellular adhesion molecule 5 (ICAM 5) and Tenacin C (Tenc) were increased in in vivo SVZ tissue, and in cultured SVZ neurospheres (Table 2 and 3).

Compared with normal SVZ tissue, MCAo dramatically induced transforming growth factor-β signaling related molecules, including Bmp6, Bmp8a, Bmpr1a, Bmpr2 and Nodal expression (Table 2). In contrast, upregulation of TGF- β genes was not detected in MCAo derived neural progenitor cells cultured in the growth medium.

The wingless (Wnt) is a large family of secreted glycoproteins and plays a key role in cell fate specification and CNS patterning (Ciani and Salinas, 2005). Frizzled (Fzd) 1, Fzd3, Fzd8,

Catna 1 and Catna 2 were upregulated in stroke SVZ tissue, but not in cultured stroke neural progenitor cells (Table 2).

Confirmation of gene expression profile by Real-Time RT-PCR and immunohistochemistry

To verify stroke-upregulated genes observed in microarrays, we performed real-time RT-PCR analysis for 21 selective genes (Table 1) in SVZ tissue and neurospheres. Upregulation of these genes was detected in MCAo SVZ tissues and cultured SVZ cells compared with that in normal SVZ cells (Fig. 1C, 1E, 2A and 2B), confirming our findings in the microarrays. Immunostaining analysis showed significant ($P<0.05$) increases of the ipsilateral SVZ cell immunoreactivity of Bmp8a (27.8 ± 5.1% vs 21.1 ± 4.3% for contralateral, n=8), integrin αV (37.5 ± 4.2% vs 18.1 ± 9.4% for contralateral, n=8), and sox 4 (15.0 ± 1.2% vs 9.4 ± 2.6% for contralateral, n=8), which are consistent with our previous findings (Liu et al., 2006). MCAo also resulted in a significant increase of tenascin C positive SVZ cells and double immunofluorescent staining revealed that these cells were GFAP immunoreactive (Fig. 3A to 3F).

Discussion

Using a customized microarray approach, genes that mediate neurogenesis and angiogenesis were screened in adult SVZ progenitor cells in vivo and in vitro after MCAo. Gene profiles in normal SVZ progenitor cells are generally consistent with previous in vivo and in vitro findings (Gurok et al., 2004;Pennartz et al., 2004;Lim et al., 2006). Ischemic stroke triggered many genes in the adult SVZ cells, which are involved in multiple signaling pathways during embryogenesis. These genes included: 1) TGF-beta1 and Bmp superfamily, 2) Wnt family, 3) Notch signals, suggesting that embryonic molecular morphogenes and signals might mediate stroke-induced neurogenesis in the adult SVZ niche (Alvarez-Buylla and Lim., 2004;Van et al., 2005;Sun et al., 2005;James et al., 2005;Bonnert et al., 2006). These gene profiles triggered by stroke may be specific to SVZ cells because in the ischemic cortex and subcortex, stroke upregulates many genes associated with stress, inflammation, apoptosis, trophic factors and immediate early genes (Soriano et al., 2000;Raghavendra et al., 2002;Lu et al., 2004;Vikman and Edvinsson., 2006).

To examine gene profile changes in vivo and in vitro after stroke, we employed SVZ tissue and a neurosphere assay that has been commonly used for studying neurogenesis in vitro (Zhang et al., 2004a;Reynolds and Weiss., 1992;Chiasson et al., 1999;Morshead et al., 2002). The gene profiles of SVZ tissue dissected 7 days after stroke have much in common with the profiles of stroke SVZ cells isolated by laser capture microdissection (Liu et al., 2006). The 7 day time point is the peak stage of neurogenesis in the SVZ cell population after stroke (Zhang et al., 2004a). Stroke upregulated more genes in SVZ tissue than that in the SVZ neurosphere cells cultured in the growth medium, which is expected because the cell population of SVZ tissue is different from that of neurosphere cells which only contain type A, B, and C cells (Alvarez-Buylla and Lim., 2004) where SVZ tissue contains SVZ neural progenitor cells, endothelial cells and microglial cells. Furthermore, neural progenitor cells in SVZ tissue are in different stages of proliferation, differentiation, and migration, which are regulated by a variety of genes, whereas neurospheres employed in the present study were cultured in the growth medium containing high levels of exogenous EGF and bFGF that propagate neurospheres, likely leading to remarkable alterations in their transcriptional profiles (Hack et al., 1993;Gabay et al., 2003;Bonnert et al., 2006).

Our observation that stroke-increased expression of MMP2 and Timp1 is intriguing, based on the emerging data that MMPs and TIMPs are involved in neurogenesis and neuroblast migration (Tsukatani et al., 2003;Yong VW, 2005;Lee et al., 2006;Zhang et al., 2006). MMPs regulate cell migration and invasion (Hu et al., 2006). Neuroblasts in the SVZ of adult rodent

travel the rostral migratory stream (RMS), as chains through tunnels formed by astrocytes, to the olfactory bulb where they differentiate into granule and periglomerular neurons throughout adult life (Garcia-Verdugo et al., 1998). Stroke increases the migration speed of neuroblasts and induces neuroblast migration towards the ischemic boundary region (Jin et al., 2003;Zhang et al., 2004a). Thus, increased expression of MMP2 and Timp1 in SVZ cells might promote neuroblast migration. In addition, stroke upregulated tenascin C expression, which mediates neuroblast migration (Peretto et al., 2005).

Although there were discrepancies of gene profile changes in neurospheres and their in vivo counterparts, eight genes upregulated by MCAo overlapped in SVZ tissue and neurospheres, suggesting that cultured SVZ cells retain signals initiated by stroke. Among them, Hif 1 α was strongly upregulated, suggesting that SVZ cells are subjected to hypoxia which could trigger changes of gene profiles (Zhu et al., 2005). Interestingly, when SVZ cells derived from MCAo mice were incubated under normal oxygen conditions, Hif 1α expression was still upregulated in these cells. Our findings are consistent with recent reports that dynamic gene profile changes were found in neurospheres cultured in different media and that SVZ cells remain stable in vitro after brain injury (Gurok et al., 2004,Dizon et al., 2006;Dictuset al., 2007). Therefore, in vivo and in vitro gene profile changes after stroke are complementary, but not identical.

In summary, we provide a dataset in comparison of in vivo and vitro gene expression changes in the adult neural progenitor cells after stroke. Our data show that stroke induces complex gene profile changes in the SVZ niche, which could serve as an initial step for future analysis of the molecular signals that mediate adult neurogenesis after stroke.

Acknowledgements

We are grateful to Cindi Roberts who provided the technical support for immunohistochemistry. This work was supported by NINDS grants PO1 NS23393, PO1 NS42345, RO1NS38292 and RO1HL 6476.

REFERENCES

Alvarez-Buylla A, Lim DA. For the long run: maintaining germinal niches in the adult brain. Neuron 2004;41:683–686. [PubMed: 15003168]

Arvidsson A, Collin T, Kirik D, Kokaia Z, Lindvall O. Neuronal replacement from endogenous precursors in the adult brain after stroke. Nat Med 2002;8:963–970. [PubMed: 12161747]

Bonnert TP, Bilsland JG, Guest PC, Heavens R, McLaren D, Dale C, Thakur M, McAllister G, Munoz-Sanjuan I. Molecular characterization of adult mouse subventricular zone progenitor cells during the onset of differentiation. Eur J Neurosci 2006;24:661–675. [PubMed: 16930398]

Chiasson BJ, Tropepe V, Morshead CM, van der Kooy D. Adult mammalian forebrain ependymal and subependymal cells demonstrate proliferative potential, but only subependymal cells have neural stem cell characteristics. J Neurosci 1999;19:4462–4471. [PubMed: 10341247]

Campos AH, Zhao Y, Pollman MJ, Gibbons GH. DNA microarray profiling to identify angiotensin-responsive genes in vascular smooth muscle cells: potential mediators of vascular disease. Circ Res 2003;92:111–118. [PubMed: 12522128]

Campos LS. Beta1 integrins and neural stem cells: making sense of the extracellular environment. Bioessays 2005;27:698–707. [PubMed: 15954093]

Ciani L, Salinas PC. WNTs in the vertebrate nervous system: from patterning to neuronal connectivity. Nat Rev Neurosci 2005;6:351–362. [PubMed: 15832199]

Dictus C, Tronnier V, Unterberg A, Herold-Mende C. Comparative analysis of in vitro conditions for rat adult neural progenitor cells. J Neurosci Methods. Jan 4;2007 online

Dizon ML, Shin L, Sundholm-Peters NL, Kang E, Szele FG. Subventricular zone cells remain stable in vitro after brain injury. Neuroscience 2006;142:717–725. [PubMed: 16935433]

Gabay L, Lowell S, Rubin LL, Anderson DJ. Deregulation of dorsoventral patterning by FGF confers trilineage differentiation capacity on CNS stem cells in vitro. Neuron 2003;40:485–499. [PubMed: 14642274]

Garcia-Verdugo JM, Doetsch F, Wichterle H, Lim DA, Alvarez-Buylla A. Architecture and cell types of the adult subventricular zone: in search of the stem cells. J Neurobiol 1998;36:234–248. [PubMed: 9712307]

Gurok U, Steinhoff C, Lipkowitz B, Ropers HH, Scharff C, Nuber UA. Gene expression changes in the course of neural progenitor cell differentiation. J Neurosci 2004;24:5982–6002. [PubMed: 15229246]

Hack N, Sue-A-Quan A, Mills GB, Skorecki KL. Expression of human tyrosine kinase-negative epidermal growth factor receptor amplifies signaling through endogenous murine epidermal growth factor receptor. J Biol Chem 1993;268:26441–26446. [PubMed: 8253771]

Hu B, Jarzynka MJ, Guo P, Imanishi Y, Schlaepfer DD, Cheng SY. Angiopoietin 2 induces glioma cell invasion by stimulating matrix metalloprotease 2 expression through the alphavbeta1 integrin and focal adhesion kinase signaling pathway. Cancer Res 2006;66:775–783. [PubMed: 16424009]

James D, Levine AJ, Besser D, Hemmati-Brivanlou A. TGFbeta/activin/nodal signaling is necessary for the maintenance of pluripotency in human embryonic stem cells. Development 2005;132:1273–1282. [PubMed: 15703277]

Jin K, Sun Y, Xie L, Peel A, Mao XO, Batteur S, Greenberg DA. Directed migration of neuronal precursors into the ischemic cerebral cortex and striatum. Mol. Cell. Neurosci 2003;24:171–189. [PubMed: 14550778]

Lee SR, Kim HY, Rogowska J, Zhao BQ, Bhide P, Parent JM, Lo EH. Involvement of matrix metalloproteinase in neuroblast cell migration from the subventricular zone after stroke. J Neurosci 2006;26:3491–3495. [PubMed: 16571756]

Lim DA, Suarez-Farinas M, Naef F, Hacker CR, Menn B, Takebayashi H, Magnasco M, Patil N, Alvarez-Buylla A. In vivo transcriptional profile analysis reveals RNA splicing and chromatin remodeling as prominent processes for adult neurogenesis. Mol Cell Neurosci 2006;31:131–148. [PubMed: 16330219]

Liu XS, Zhang ZG, Zhang RL, Gregg S, Morris DC, Wang Y, Chopp M. Stroke induces gene profile changes associated with neurogenesis and angiogenesis in adult subventricular zone progenitor cells. J Cereb Blood Flow Metab. 2006In press

Livak KJ, Schmittgen TD. Analysis of relative gene expression data using real-time quantitative PCR and the $2^{-\Delta\Delta Ct}$ method. Methods 2001;25:402–408. [PubMed: 11846609]

Lu XC, Williams AJ, Yao C, Berti R, Hartings JA, Whipple R, Vahey MT, Polavarapu RG, Woller KL, Tortella FC, Dave JR. Microarray analysis of acute and delayed gene expression profile in rats after focal ischemic brain injury and reperfusion. J Neurosci Res 2004;77:843–857. [PubMed: 15334602]

Morshead CM, Benveniste P, Iscove NN, van der Kooy D. Hematopoietic competence is a rare property of neural stem cells that may depend on genetic and epigenetic alterations. Nat Med 2002;8:268–273. [PubMed: 11875498]

Parent JM, Vexler ZS, Gong C, Derugin N, Ferriero DM. Rat forebrain neurogenesis and striatal neuron replacement after focal stroke. Ann. Neurol 2002:802–813. [PubMed: 12447935]

Pennartz S, Belvindrah R, Tomiuk S, Zimmer C, Hofmann K, Conradt M, Bosio A, Cremer H. Purification of neuronal precursors from the adult mouse brain: comprehensive gene expression analysis provides new insights into the control of cell migration, differentiation, and homeostasis. Mol Cell Neurosci 2004;25:692–706. [PubMed: 15080897]

Peretto P, Giachino C, Aimar P, Fasolo A, Bonfanti L. Chain formation and glial tube assembly in the shift from neonatal to adult subventricular zone of the rodent forebrain. J Comp Neurol 2005;487:407–427. [PubMed: 15906315]

Raghavendra Rao VL, Bowen KK, Dhodda VK, Song G, Franklin JL, Gavva NR, Dempsey RJ. Gene expression analysis of spontaneously hypertensive rat cerebral cortex following transient focal cerebral ischemia. J Neurochem 2002;83:1072–1086. [PubMed: 12437578]

Ran R, Xu H, Lu A, Bernaudin M, Sharp FR. Hypoxia preconditioning in the brain. Dev Neurosci 2005;27:87–92. [PubMed: 16046841]

Reynolds BA, Weiss S. Generation of neurons and astrocytes from isolated cells of the adult mammalian central nervous system. Science 1992;255:1707–1710. [PubMed: 1553558]

Sharp FR, Ran R, Lu A, Tang Y, Strauss KI, Glass T, Ardizzone T, Bernaudin M. Hypoxic preconditioning protects against ischemic brain injury. NeuroRx 2004;1:26–35. [PubMed: 15717005]

Soriano MA, Tessier M, Certa U, Gill R. Parallel gene expression monitoring using oligonucleotide probe arrays of multiple transcripts with an animal model of focal ischemia. J Cereb Blood Flow Metab 2000;20:1045–1055. [PubMed: 10908038]

Sun Y, Lowther W, Kato K, Bianco C, Kenney N, Strizzi L, Raafat D, Hirota M, Khan NI, Bargo S, Jones B, Salomon D, Callahan R. Notch4 intracellular domain binding to Smad3 and inhibition of the TGF-beta signaling. Oncogene 2005;24:5365–5374. [PubMed: 16007227]

Tsukatani T, Fillmore HL, Hamilton HR, Holbrook EH, Costanzo RM. Matrix metalloproteinase expression in the olfactory epithelium. Neuroreport 2003;14(8):1135–1140. [PubMed: 12821796]

van Es JH, van Gijn ME, Riccio O, van den Born M, Vooijs M, Begthel H, Cozijnsen M, Robine S, Winton DJ, Radtke F, Clevers H. Notch/gamma-secretase inhibition turns proliferative cells in intestinal crypts and adenomas into goblet cells. Nature 2005;435:959–963. [PubMed: 15959515]

Vikman P, Edvinsson L. Gene expression profiling in the human middle cerebral artery after cerebral ischemia. Eur J Neurol 2006;13:1324–1332. [PubMed: 17116215]

Yong VW. Metalloproteinases: mediators of pathology and regeneration in the CNS. Nat Rev Neurosci 2005;6:931–944. [PubMed: 16288297]

Zhang R, Zhang Z, Wang L, Wang Y, Gousev A, Zhang L, Ho KL, Morshead C, Chopp M. Activated neural stem cells contribute to stroke-induced neurogenesis and neuroblast migration toward the infarct boundary in adult rats. J. Cereb. Blood. Flow. Metab 2004a;24:441–448. [PubMed: 15087713]

Zhang R, Zhang Z, Zhang C, Zhang L, Robin A, Wang Y, Lu M, Chopp M. Stroke transiently increases subventricular zone cell division from asymmetric to symmetric and increases neuronal differentiation in the adult rat. J. Neurosci 2004b;24:5810–5815. [PubMed: 15215303]

Zhang RL, Chopp M, Zhang ZG, Jiang Q, Ewing JR. A rat model of embolic focal cerebral ischemia. Brain Research 1997;766:83–92. [PubMed: 9359590]

Zhang RL, Zhang ZG, Zhang L, Chopp M. Proliferation and differentiation of progenitor cells in the cortex and the subventricular zone in the adult rat after focal cerebral ischemia. Neuroscience 2001;105:33–41. [PubMed: 11483298]

Zhang Z, Davies K, Prostak J, Fenstermacher J, Chopp M. Quantitation of microvascular plasma perfusion and neuronal microtubule-associated protein in ischemic mouse brain by laser-scanning confocal microscopy. J. Cereb. Blood. Flow. Metab 1999;19:68–78. [PubMed: 9886357]

Zhang RL, Zhang ZG, Chopp M. Neurogenesis in the adult ischemic brain: generation, migration, survival, and restorative therapy. Neuroscientist 2005;11:408–416. [PubMed: 16151043]

Zhang ZG, Letourneau Y, Zhang RL, Gregg SR, Hozeska A, Wang Y, Morris D, Chopp M. Atypical PKC ζ mediates neuroblast migration from the subventricular zone toward the ischemic boundary regions. Stroke 2006;37:629.

Zhu LL, Wu LY, Yew DT, Fan M. Effects of hypoxia on the proliferation and differentiation of NSCs. Mol Neurobiol 2005;31:231–242. [PubMed: 15953824]

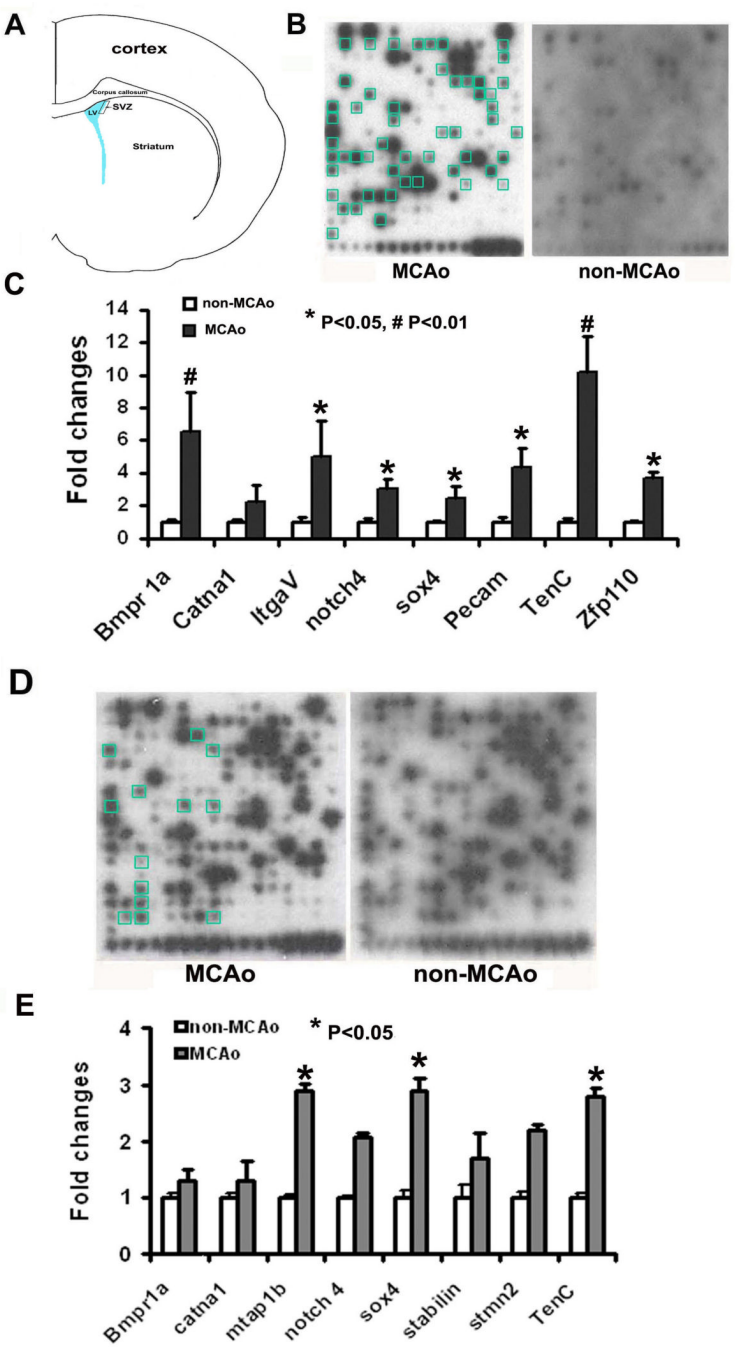

Figure 1.

A schematic of a coronal brain section shows a box where SVZ tissue was harvested for microarray analysis and the ependymal cells were not included (A). Total RNAs obtained from SVZ tissue of normal mice or mice subjected to 7 day MCAo were extracted and microarray was performed by means of the non-radioactive GEArray Q series cDNA expression array filters. Panel B shows gene profiles of GE mouse stem cell cDNA chip from representative stroke and non-stroke SVZ tissues. Real-time RT-PCR analysis confirmed selective upregulated-genes detected on the microarrays in SVZ tissue (C). Panel D shows gene profiles of cultured SVZ cells harvested from normal mice and mice subjected from MCAo. Panel E shows real-time RT-PCR results of selective upregulated-genes in cultured SVZ cells. SVZ

cells were cultured in the growth medium for 7 days. Blue boxes in panels B (MCAo) and D (MCAo) represent upregulated genes. *P<0.05, #P<0.01, n=5-6 /group, LV = lateral ventricle.

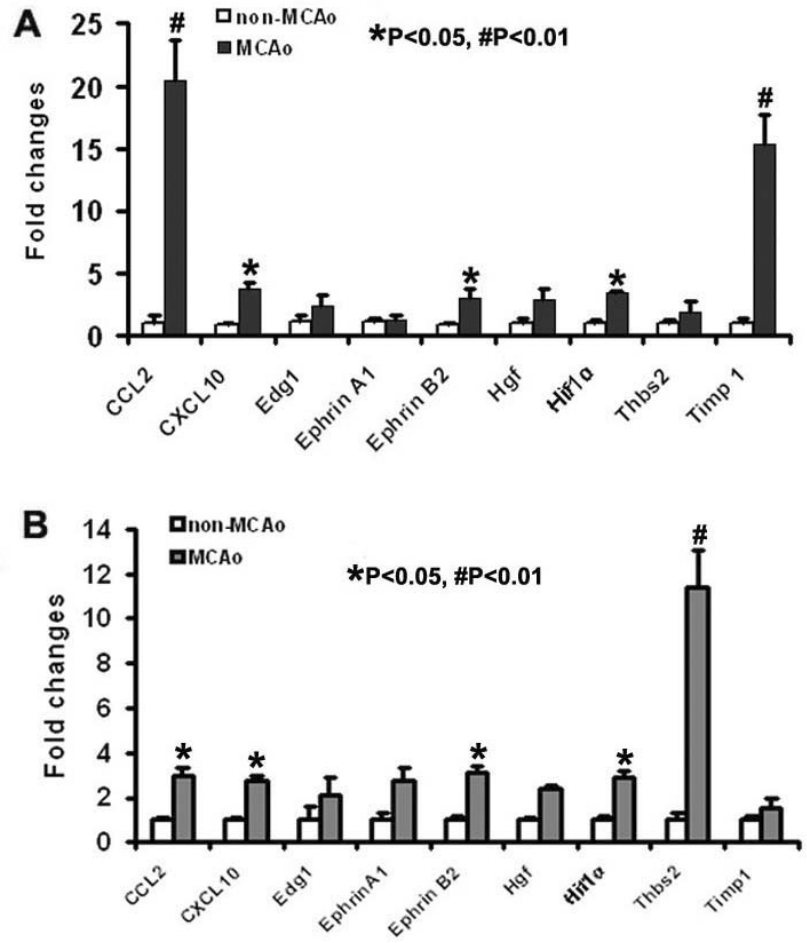

Figure 2.

Panels A and B are the results of real-time RT-PCR analysis showing mRNA levels of selective genes that were upregulated on the Oligo GEArray Mouse Angiogenesis microarray in SVZ tissue (A) and cultured SVZ neuropsheres (B). *P<0.05, #P<0.01, n=5-6 /group.

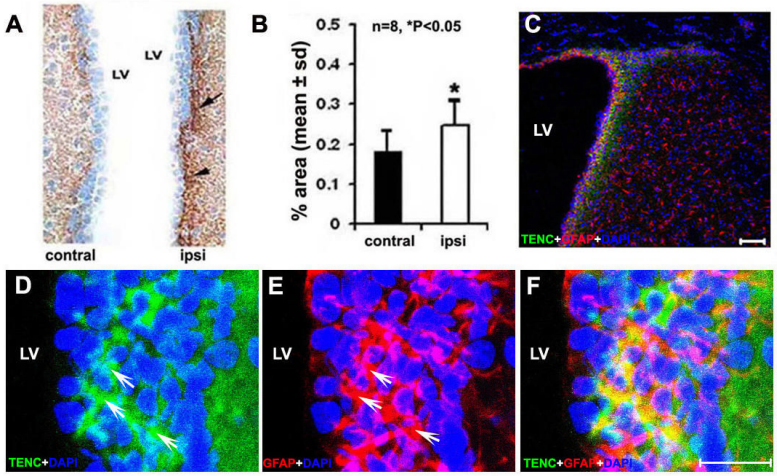

Figure 3.

Microphotographs of tenascin C immunoreactive cells in the SVZ. MCAo induced an increase in tenascin C immunoreactive cells in the ipsilateral SVZ (A, ipsi), although tenascin C immunoreactive cells were presented in the contralateral SVZ (A, contral). Panel B shows semi-quantitative data of tenascin C immunoreactivity. Double immunofluorescent staining revealed that tenascin C (TENC) immunoreactive cells (C, D and F, arrows) were GFAP positive (E and F, arrows). LV = lateral ventricle.

Table 1

Primer sequences of genes applied in real-time RT-PCR

Genes	Sense	Anti-sense	Size
β-actin	5′-CCATCATGAAGTGTGACGTTG	5′-CAATGATCTTGATCTTCATGGTG	150bp
Bmpr1a	5′-ATGCAAGGATTCACCGAAAG	5′-AACAACAGGGGGCAGTGTAG	100bp
Catna1	5′-CTACGTGGCTTCCACCAAAT	5′-TCTCTTCACCAACGGCTTCT	109bp
CCL2	5′-CCCAATGAGTAGGCTGGAGA	5′-TCTGGACCCATTCCTTCTTG	125bp
CXCL 10	5′-AAGTGCTGCCGTCATTTTCT	5′-CTATGGCCCTCATTCTCAC	128bp
Edg1	5′-GGCCCCTCTCTTCATCCTAC	5′-GATGATGGGGTTGGTACCTG	124bp
Ephrin A1	5′-ATCAGGAATCCCAGTGC TG	5′-CAATGCTGTGCAAAACCTGT	134bp
Ephrin B2	5′-AATCTCCTGGGTTCCGAAGT	5′-GTCTCCTGCGGTACTTGAGC	111bp
Hgf	5′-AGGAACAGGGGCTTTACGTT	5′-GTCAAATTCATGGCCAAACC	126bp
Hif1α	5′-GAAATGGCCCAGTGAGAAAA	5′-CTTCCACGTTGCTGACTTGA	119bp
Mtap 1b	5′-AACCTCATCTCCCCTGACCT	5′-TGTTGGGTTCTGGGTCTTTC	73bp
Notch4	5′-GCTCTTGCCACTCAATTTCC	5′-GAGATAGCCTCAGGCAGGTG	101bp
PECAM	5′-TCACCATCAACAGCATCCAT	5′-GGTGCTGAGACCTGCTTTTC	120bp
Stmn2	5′-GCAATGGCCTACAAGGAAAA	5′-TTCACCTCCATGTCGTCGTA	116bp
Stabilin 1	5′-ACCTGTCATGGGAGAGTTGG	5′-ACAGTGAAAGGTCCGTCACC	110bp
Sox4	5′-AGTGAAGCGCGTCTACCTGT	5′-TTCGTACAACCCCAGTGGAT	102bp
TenC	5′-TGGAGTACGAGCTGCATGAC	5′-AAACTTGGTGGCGATGGTAG	101bp
Thbs2	5′-GTGATGTCACCAGCAACACC	5′-CAAGTCACGGAGCATGAAGA	135bp
Timp 1	5′-CATGGAAAGCCTCTGTGGAT	5′-AAGAAGCTGCAGGCATTGAT	111bp
Zfp110	5′-CAGAAGGGCACTGGAAAGAG	5′-TATGGAGGAGCCATGTGTCA	141bp

Table 2

Gene expression profile in subventricular zone tissues after MCAo

Symbol	Gene name	RefSeq number	Fold change
Angptl4	Angiopoietin-like 4	NM_020581	1.53
Bmp6	Bone morphogenetic protein 6	NM_007556	1.82
Bmp8a	Bone morphogenetic protein 8a	NM_007558	1.88
Bmpr1a	Bone morphogenetic protein receptor, type 1A	NM_009758	1.62
Bmpr2	Bone morphogenic protein receptor, type II (serine/threonine kinase)	NM_007561	2.01
Catna1	Catenin alpha 1	NM_009818	2.07
Catna2	Catenin alpha 2	NM_009819	1.67
CCL2*	Chemokine (C-C motif) ligand 2	NM_011333	2.99
Cd34	CD34 antigen	NM_133654	2.46
CXCL10*	Chemokine (C-X-C motif) ligand 10	NM_021274	9.92
Cst3	Cystatin C	NM_009976	2.26
Erbb2ip	Erbb2 interacting protein	NM_021563	1.95
Fgf12	Fibroblast growth factor 12	NM_010199	1.94
Fgf22	Fibroblast growth factor 22	NM_023304	1.97
Fgf23	Fibroblast growth factor 23	NM_022657	2.30
Fgf3	Fibroblast growth factor 3	NM_008007	2.32
Fgf5	Fibroblast growth factor 5	NM_010203	3.11
Fgfr1	Fibroblast growth factor receptor 1	NM_010206	2.39
Fzd1	Frizzled homolog 1 (Drosophila)	NM_021457	2.58
Fzd3	Frizzled homolog 3 (Drosophila)	NM_021458	1.68
Fzd8	Frizzled homolog 8 (Drosophila)	NM_008058	2.09
Gata2*	GATA binding protein 2	NM_008090	1.62
Gcm2	Glial cells missing homolog 2 (Drosophila)	NM_008104	1.59
Gdf9	Growth differentiation factor 9	NM_008110	2.36
Gjb1*	Gap junction membrane channel protein beta 1	NM_008124	1.96
Hif1 α*	Hypoxia inducible factor 1, alpha subunit	NM_010431	2.29
Icam5*	Intercellular adhesion molecule 5, telencephalin	NM_008319	1.92
Il6st	Interleukin 6 signal transducer	NM_010560	3.10
Itga6	Integrin alpha 6	NM_008397	1.95
Itga7	Integrin alpha 7	NM_008398	3.19
Itgav	Integrin alpha V	NM_008402	4.23
Itgax	Integrin alpha X	NM_021334	3.18
Itgb4	Integrin beta 4	L04678	2.03
Lifr	Leukemia inhibitory factor receptor	NM_013584	2.92
Mmp2	Matrix metalloproteinase 2	NM_008610	1.63
Mbp	Myelin basic protein	NM_010777	2.41
Mtap2	Microtubule-associated protein 2	NM_008632	2.35
Mtap1b	Microtubule-associated protein 1 B	NM_008634	1.57
Myl4	Myosin, light polypeptide 4, alkali; atrial, embryonic	NM_010858	1.84
Ncam2	Neural cell adhesion molecule 2	NM_010954	2.44
Nefl	Neurofilament, light polypeptide	NM_010910	3.05
Nkx2-2	NK2 transcription factor related, locus 2 (Drosophila)	NM_010919	3.38
Nodal	Nodal	NM_013611	2.04
Notch4	Notch gene homolog 4 (Drosophila)	NM_010929	1.99
Ntrk2	Neurotrophic tyrosine kinase, receptor, type 2	NM_008745	3.43
Olig1	Oligodendrocyte transcription factor 1	NM_016968	2.86
Plp	Proteolipid protein (myelin)	NM_011123	1.55
Prdc	Protein related to DAN and cerberus	NM_011825	2.31
Ptch	Patched homolog	NM_008957	1.75
Stmn2	Stathmin-like 2	NM_025285	3.36
Slc1a2	Solute carrier family 1, member 2	NM_011393	2.19
Sox3	SRY-box containing gene 3	NM_009237	2.79
Sox4*	SRY-box containing gene 4	NM_009238	2.39
Sphk1	Sphingosine kinase 1	NM_025367	1.93
Stab1	Stabilin 1	NM_138672	2.14
Timp1*	Tissue inhibitor of metalloproteinase 1	NM_011593	2.85
Utf1	Undifferentiated embryonic cell transcription factor 1	NM_009482	2.04
Zfp110	Zinc finger protein 110	NM_022981	3.99

* shows the upregulated-genes were detected on microarrays in both SVZ tissue and SVZ neuropsheres.

Table 3

Gene expression alteration in subventricular zone neurospheres after MCAo

Symbol	Gene name	RefSeq number	Fold change
CCL2*	Chemokine (C-C motif) ligand 2	NM_011333	2.21
Cdkn1a	Cyclin-dependent kinase inhibitor 1A (P21)	NM_007669	1.65
Ctgf	Connective tissue growth factor	NM_010217	1.77
CXCL10*	Chemokine (C-X-C motif) ligand 10	NM_021274	2.95
Dnmt1	DNA methyltransferase (cytosine-5) 1	NM_010066	1.95
Edg1	Endothelial differentiation sphingolipid G-protein-coupled receptor 1	NM_007901	2.75
Efnb2	Ephrin B2	NM_010111	3.27
Egfr	Epidermal growth factor receptor	NM_007912	1.51
Gata2*	GATA binding protein 2	NM_008090	2.49
Gjb1*	Gap junction membrane channel protein beta 1	NM_008124	1.52
Hgf	Hepatocyte growth factor	XM_131908	4.92
Hif1α*	Hypoxia inducible factor 1, alpha subunit	NM_010431	3.47
Icam5*	Intercellular adhesion molecule 5, telencephalin	NM_008319	1.81
Igf1r	Insulin-like growth factor I receptor	NM_010513	1.60
Notch1	Notch gene homolog 1 (Drosophila)	NM_008714	1.89
Pofut1	Protein O-fucosyltransferase 1	NM_080463	1.67
S100b	S100 protein, beta polypeptide, neural	NM_009115	1.68
Sox4*	SRY-box containing gene 4	NM_009238	1.76
Thy1	Thymus cell antigen 1, theta	NM_009382	2.16
Thbs2	Thrombospondin 2	NM_011581	1.81
Timp1*	Tissue inhibitor of metalloproteinase 1	NM_011593	1.89
Tenc	Tenascin C	NM_011607	3.46
Vim	Vimentin	NM_011701	1.59

* shows the upregulated-genes were detected on microarrays in both SVZ tissue and SVZ neuropsheres.